Electron Addition to Trimethylphosphine Sulfide

S. P. Mishra

Nuclear and Radiation Chemistry Laboratory, Department of Chemistry, Banaras Hindu University, Varanasi 221 005, India

M. C. R. Symons*

Department of Chemistry, DeMontfort University, The Gateway, Leicester, LE1 9BH, U.K.

Received: July 1, 1997[⊗]

Exposure of dilute solutions of trimethylphosphine sulfide (Me_3PS) in methanol (CD_3OD)−water glasses to ionizing radiation at 77 K gave the parent radical anion Me_3PS^-, identified by its EPR spectrum. This is shown to have a trigonal bipyramidal structure characteristic of phosphoranyl radicals. Similar features were obtained for the pure compound at 77 K, with resolved proton splitting on the parallel features from one CH_3 group. Doublet features assigned to the parent cations, $Me_3P-\dot{S}^+$ were observed for solutions in freon ($CFCl_3$) and also in the pure compound. The latter also gave features assigned to $H_2\dot{C}P(Me_2)S$ and/or $H_2\dot{C}P(Me)_2$-SH^+ radicals. On annealing to *ca*. 140 K, doublet features with a considerably reduced ^{31}P hyperfine splitting, assigned to the phosphoryl radical $Me_2\dot{P}S$, were revealed for the pure compound. At 77 K, these features were further split into 1:2:1 triplets, apparently from only two equivalent protons. However, at *ca*. 140 K, septets from all six protons were obtained with almost the same separation between the outmost features. Also, the original ^{31}P parallel and perpendicular features gave way to features that had converged, although some anisotropy was still seen. At still higher temperatures, an isotropic doublet of septets was observed, prior to loss of the features. This is assigned to freely rotating $Me_2\dot{P}S$ radicals. Possible mechanisms for the formation of these $Me_2\dot{P}S$ radicals are discussed. The only reasonable one that we can discover is electron return to give electronically excited $(Me_3PS)^*$ molecules, which dissociate to give $\dot{C}H_3$ and $Me_2\dot{P}S$ radicals. The former radicals ($\dot{C}H_3$) were not detected, but they may well react to give methane and the $H_2\dot{C}P(Me)_2S$ radical. The reversible change from 3 to 7 lines from the two methyl groups in $Me_2\dot{P}S$ radicals is discussed in terms of hindered rotation for the two methyl groups.

Introduction

By working at low temperatures, matrix-isolated radicals generated by ionizing radiation can be transformed into intermediates that have clear relevance to liquid-phase kinetic studies. A nice example of this is the recent mechanistic study of Breslow and co-workers[1] who had the insight to postulate the formation of a 3-electron or σ^* intermediate. This was later formed and studied by EPR spectroscopy in the solid state, thereby strongly supporting this postulate.[2] The present study was specifically undertaken in the expectation that it would help to pull together some of the major recent discoveries in this field. We selected phosphorus since phosphorus derivatives have been extremely useful because of the distinctive doublet hyperfine splittings from ^{31}P, which are often large and readily detectable. Hence, radicals of type $\dot{P}L_4$ (usually described as phosphoranyl radicals), $\dot{P}L_3$ (phosphoryl radicals), and $\dot{P}L_2$ (phosphinyl radicals) have been thoroughly investigated both in solution[3] and especially in the solid state.[4] Also, radicals in which the SOMO is largely confined to various ligands have been widely studied.[5] In the course of our own work on these species we found that there was a very marked tendency for the formation of σ^* dimer for radicals, as shown in reaction 1.[6]

$$PL_3^+ + :PL_3 \rightarrow L_3P\text{-}\dot{\cdot}\text{-}PL_3^+ \qquad (1)$$

These dimers are usually described as σ^*- or 3-electron radicals. It is now realized that such σ^* intermediates can be of great importance in reaction mechanisms involving radicals.[1]

Such studies, in addition to helping to probe the reactions of phosphorus radical species, have, in our view, shed light on a number of issues that have far more general significance. Since species containing P−S bonds have not been widely studied in this way, we decided to investigate the radiation chemistry of Me_3PS, which has not been previously studied using these techniques. Our aims were to prepare a range of these types of radicals from Me_3PS, using ionizing radiation, and hence to obtain data that could highlight the wider issues. These include the tendency to form σ^* adducts, the presence of double bonds such as $Me_3P{=}S$, and the reasons for the pyramidal characters of phosphoryl and related radicals.

In addition to studying the effects of ionizing radiation on the pure compound, we probed specific electron loss using $CFCl_3$ as solvent and specific electron capture using CD_3OD as solvent. The former solvent captures ejected electrons irreversibly with high efficiency, but the solvent electron-loss centers ($CFCl_3^+$) migrate by e^- transfer to solutes, S, to give $\dot{S}^+$.[7] In contrast, methanol (CD_3OD is used to minimize interference from solvent radical signals) captures the e^--loss centers, giving $\dot{C}D_2OD$, but does not react efficiently with e^- which can therefore reach the solute to give $\dot{S}^-$ centers specifically.[8]

Experimental Section

Trimethylphosphine sulfide (Strem) and $CFCl_3$ (BDH) were the highest grades available and used as received. The pure material, as very fine powder, was irradiated at room temperature or 77 K with ^{60}Co Y-rays or with 1.5 keV ($2.4 \times 10^{1-6}$J) X-rays to doses upto 10 kGy (the results were independent of dose).

* Corresponding author.
⊗ Abstract published in *Advance ACS Abstracts,* September 15, 1997.

S1089-5639(97)02135-X CCC: $14.00

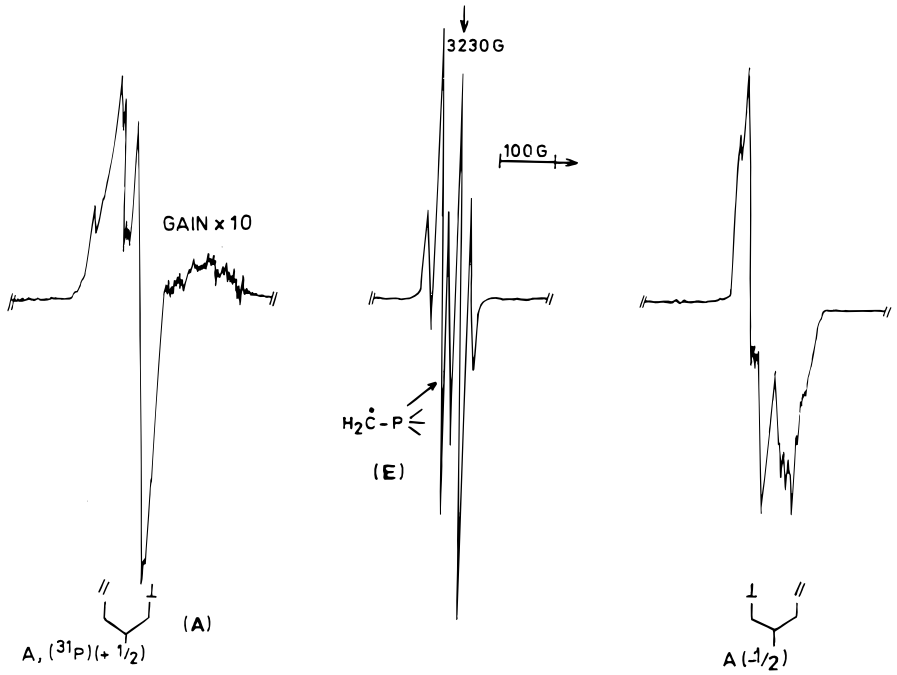

Figure 1. First-derivative X-band EPR spectrum of trimethylphosphine sulfide after exposure to ionizing radiation at 77 K, showing features assigned to $Me_3\dot{P}S$ radicals (species A, outer features) and $H_2\dot{C}P(S)Me_2$ radicals (species E, central features).

The solutions of the material in CD_3OD (as small glassy beads *ca*. 0.1 mol dm^{-3}) or in $CFCl_3$ (*ca*. 10^{-3} mol dm^{-3}) were irradiated in order to detect specific e^--gain and e^--loss centers and also to study the secondary products.

EPR spectra were normally recorded at low modulation (1−2 G) and low power (∼1 mW) on a Varian E109 X-band spectrometer using 100 kHz modulation and fitted with a frequency counter (Marconi Instruments Type 2440). This was interfaced to an Archimedes computer. All the 77 K irradiated samples were annealed in the insert Dewar, with continuous monitoring of the EPR spectra, and recooled to 77 K whenever significant changes were observed. For room temperature irradiated samples, spectra were recorded at room temperature and at 77 K.

Results

After irradiation at 77 K, the major detectable EPR features for pure Me_3PS comprised an anisotropic ^{31}P doublet (A) and central features (E) comprising a set of 5 lines (Figure 1). In addition, an extra low-field doublet together with a similar doublet in the center of the spectrum were detected (B), which became better defined on slight annealing, and which was the dominant feature using $CFCl_3$. The features for species A were also obtained using CD_3OD as solvent. There are extra small quartet splittings of *ca*. 15 G, on some of the A lines, which probably stem from one unique $-CH_3$ group.

On annealing to *ca*. 140 K a second set of ^{31}P lines (C) with slightly greater splitting than that for A grew in as those for A decayed. This center was transient and we were unable to isolate the features clearly from those for A prior to loss of both sets. At the same time, another set of lines with a smaller ^{31}P splitting grew in (D), each component appearing as a 1:2:1 triplet at 77 K (Figure 2a). Species C also grew in as a minor component on annealing the CD_3OD systems, but the D features were not seen for the solutions at any stage prior to melting.

The EPR spectra for species D changed reversibly on annealing between 77 and *ca*. 140 K (compare parts a and b of Figure 2). There are two related, but possibly independent, averaging processes involved. In one, associated with rotations of the methyl groups relative to the main frame of the radicals, the original triplet features from ^{1}H hyperfine coupling change into septets, such that the total splitting between the outer lines remains constant. These changes, which were quite reversible, are discussed below. The other change is in the anisotropy associated with the ^{31}P hyperfine features. These are partially averaged by some type of specific, hindered rotation or libration. This is such that one component of the original (77 K) $\pm^1/_2$-(^{31}P) perpendicular features (*x*) remains unaltered, while the *y* and the *z* components are averaged. The situation envisaged is shown below in Figure 4b. The resulting partially averaged spectrum has apparent perpendicular features that lie outside the new parallel features. On further warming, isotropic septet features appeared as decay of all feature set in. This is discussed below.

Discussion

Identification. *Species A*. Analysis of the derived ^{31}P hyperfine coupling constants (Table 1) gives 3s and 3p orbital populations of *ca*. 0.17 and 0.45 (Table 2). (These are based on the use of calculated atomic parameters.[9] They are widely used as a guideline to trends in structure.) These results are in good accord with expectation for normal "trigonal bipyramidal" (TBP) phosphoranyl centers, having only one electronegative apical ligand (I) (Table 1).

Species D. This is identified as the phosphoryl radical $Me_2\dot{P}S$ for two major reasons: (i) The ^{31}P hyperfine coupling data correlate well with those for related species (Table 1 and Figure 3). (ii) The septet splitting from six equivalent protons, observed on annealing, together with its magnitude (5.7 G) is in good agreement with expectation for the two methyl groups, being in fact, almost equal to that for $Me_2\dot{P}O$ radicals, which were unambiguously identified.[10]

Species B. This center, with a well-defined parallel doublet (22 G) at $g_{||} = 2.07$, and a pair of lines with almost the same splitting close to $g = 2.0036$, is identified as the parent cation, $Me_3\dot{P}S^+$, with the spin largely localized on sulfur. This is supported by the fact that the center was formed using $CFCl_3$ matrices, which strongly favor formation of the parent radical

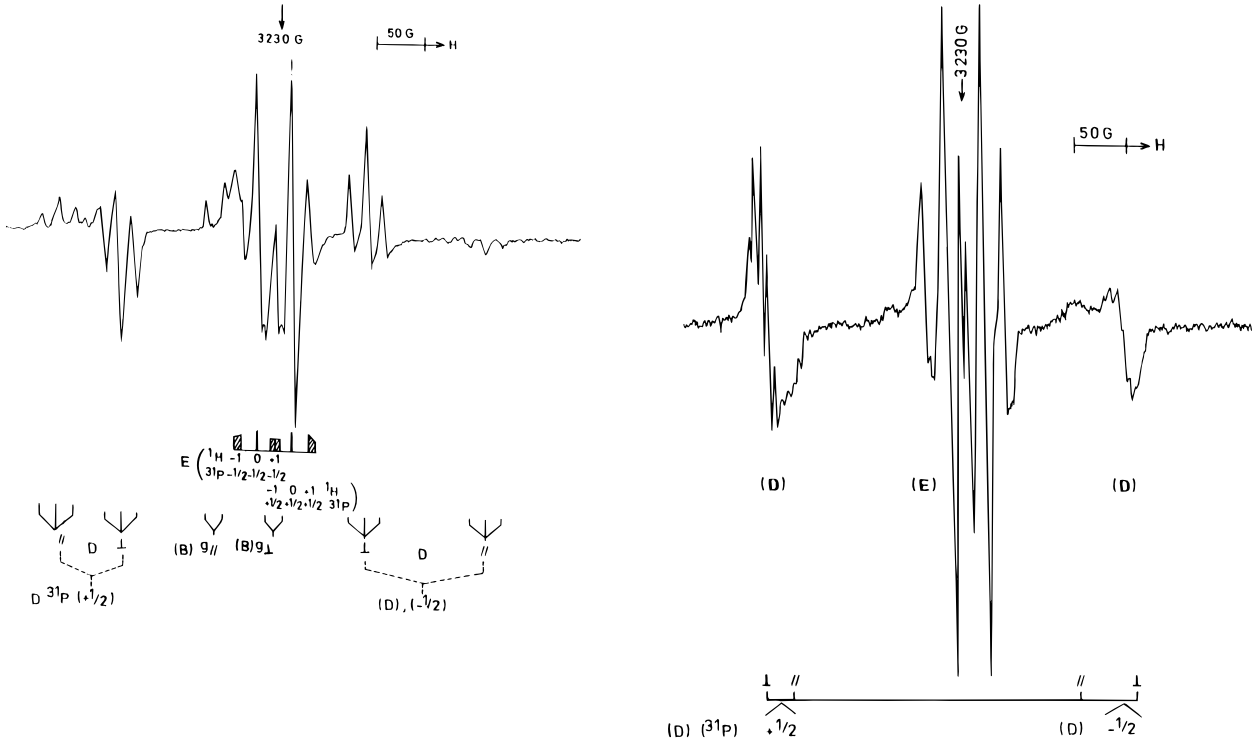

Figure 2. First-derivative X-band EPR spectrum of trimethylphosphine sulfide after exposure to ionizing radiation at 77 K and annealing to remove features assigned to $Me_3\dot{P}S^-$ radical anions (a, left) at 77 K, showing features assigned to $Me_2\dot{P}S$ radicals (species D) together with species E [$H_2\dot{C}P(S)Me_2$] (central features) and species B($Me_3\dot{P}S^+$) (b, right) at *ca.* 140 K showing the averaging of ^{1}H coupling from triplets to septets.

TABLE 1: EPR Hyperfine Coupling Constants for Various Radicals (A, B, C, D, E) Produced in Irradiated Trimethylphosphine Sulfide Together with Related Species

radicals	medium/ temp (K)	^{31}P hyperfine coupling (G)[a]			^{1}H coupling (CH_3)
		∥	⊥	iso	
$Me_3\dot{P}S^-$(A)	CD_3OD/77	710	570	616	15 (3H)
	pure/77	710	570	616	15 (3H)
$Me_3\dot{P}O^-$[b]	pure/77	738	548	611	
$Ph_3\dot{P}S^-$[c]	CD_3OD/77	620	485	530	
$Ph_3\dot{P}SH$[d]	CD_3OD/77	533	310	391	
$Me_3\dot{P}SR$ (C)	CD_3OD/77	805	700	651	
$Me_2\dot{P}S$ (D)	pure/77	450	256	321	
	ca. 140	275	345	322	5.7
$Me_2\dot{P}O$[b]	pure/77	535	295	375	
	ca. 140	433	310	375	5.6
$Me_3\dot{P}S^+$ (B)	$CFCl_3$/77	22	20	20.6[f]	
$Ph_3\dot{P}S^+$	$CFCl_3$/77	22	20	20.6[g]	
$H_2\dot{C}P(S)Me_2$ (E)	pure/77		ca. 35.5[h]		20.3 (CH_2)
$H_2\dot{C}P(O)Me_2$[b]	pure/77		ca. 38[i]		21 (CH_2)

[a] 1 G = 10^{-4} T; *A* and *g* values derived from simulations. [b] Reference 10. [c] Evans, J. C.; Mishra, S. P.; Rowlands, C. C. *Chem. Phys. Lett.* **1980**, *72*, 168. [d] Reference 16. [e] Reference 19. [f] $g_{\parallel} = 2.075$; $g_{\perp} = 2.003$. [g] $g_{\parallel} = 2.130$; $g_{\perp} = 2.002$. [h] $g \sim 2.0023$. [i] $g \sim 2.003$.

cation. The only reasonable alternative, in our view, is the σ^* dimer cation, $Me_3PS\text{-}\overset{+}{S}PMe_3$. However, this would give a triplet ^{31}P splitting and is expected to have $g_{max} \approx 2.02$, rather than 2.07, and should not have been a primary product using dilute $CFCl_3$ solutions. Nevertheless, the orbital motion arising from the two coupled 3p(π) orbitals on sulfur has been considerably quenched by some unidentified perturbation.

Species E. The central features comprise an anisotropic triplet characteristic of a $-CH_2$ group together with an isotropic doublet splitting assigned to ^{31}P. The radical is clearly either $H_2\dot{C}P(S)(CH_3)_2$ or $H_2\dot{C}P(SH)(CH_3)_2^+$. The coupling to two equivalent protons and the almost isotropic ^{31}P splitting gives clear identification. The overall spectrum closely resembles that previously assinged to $H_2\dot{C}P(O)(CH_3)_2$ radicals, for example.[10,11]

TABLE 2: Derived Orbital Populations for Phosphoranyl and Phosphoryl Radicals

radicals	orbital parameters			
	$2B$	a_s^2 (%)	a_p^2 (%)	λ^2
$Me_3\dot{P}S^-$	93	16.9	45.3	2.7
$Me_3\dot{P}O^-$	126	17.0	61.5	3.6
$Ph_3\dot{P}S^-$	90	14.0	45.0	3.2
$Ph_3\dot{P}SH$	162	10.7	78.3	7.3
$Me_3\dot{P}SR$	154	17.8	74.7	4.1
$Me_2\dot{P}S^-$	129	8.8	62.2	7.0
$Me_2\dot{P}O$	163	10.3	79.1	7.6

Aspects of Structure. *Phosphoranyl Radicals.* These are thought to have two limiting structures, one formed by the lengthening of one specific bond, leaving the unit essentially tetrahedral (I), and the other involving an increase in the angle between two of the ligands leading to the TBP structure II. (Here

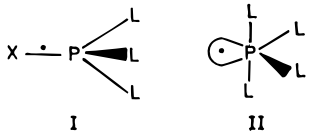

the sp hybridized orbital of the unpaired electron is often visualized as the "third" in-plane ligand.) If the symmetry is low, some compromise between these limiting structures is expected. The former are essentially σ^* radicals, the SOMO being confined largely to the stretched X−P bond, as in I. This structure is favored if there is a unique ligand (X) having a high electron affinity, relative to L.

The SOMO for the latter is an sp^n hybrid on phosphorus with relatively high spin densities on the axial ligands but very little on the equatorial pair. Hence for structure I the spin density is high on the axial $-CH_3$ group but undetectably small for the other two $-CH_3$ groups.

In contrast with the phosphoryl radicals (see Figure 3), there is no clear trend in the p/s ratio (λ^2) estimated from the ^{31}P

TABLE 3: λ_2 Value for Radicals Used in Figure 3

L	X	λ^2	ref
CH_3		9.5	*a*
C_2H_5		9.3	*a*
Ph_3		9.6	*b*
CH_3	O	7.1	*c*
CH_3	S	7.3	*d*
Ph	O	7.5	*e*
H	O	5.1	*f*
Ph	O	5.3	*g*
Ph	O, OH	5.5	*g*
	O	3.3	*h*
	OH	2.3	*i*
	O(2), OCH_3(1)	2.7	*j*
	O(1), OCH_3(2)	2.5	*k*

[a] Begum, A.; Lyons, A. R.; Symons, M. C. R. *J. Chem. Soc A* **1977**, 2290. [b] Evans, J. C.; Mishra, S. P.; Rowlands, C. C. *Chem. Phys. Lett.* **1980**, *72*, 168. [c] Begum, A.; Symons, M. C. R. *J. Chem. Soc., Faraday Trans. 2* **1973**, *69*, 43. [d] This work. [e] Geoffrey, M.; Lucken, E. A. C. *Mol. Phys.* **1971**, *22*, 257. [f] Morton, J. F. *Mol. Phys.* **1962**, *5*, 217. [g] Geoffrey, M.; Lucken, E. A. C. *Mol. Phys.* **1972**, *24*, 335. [h] Horsfield, A.; Morton, J. R.; Whitten, D. H. *Mol. Phys.* **1961**, *4*, 475. [i] Ginns, I. S.; Mishra, S. P.; Symons, M. C. R. *J. Chem. Soc., Dalton Trans.* **1973**, 2509. [j] Kerr, C. M. L.; Webster, K.; Williams, F. *Mol. Phys.* **1973**, *16*, 1461. [k] Davies, A. G.; Griller, D.; Roberts, B. P. *Angew. Chem. Int. Ed. Engl.* **1971**, *10*, 738.

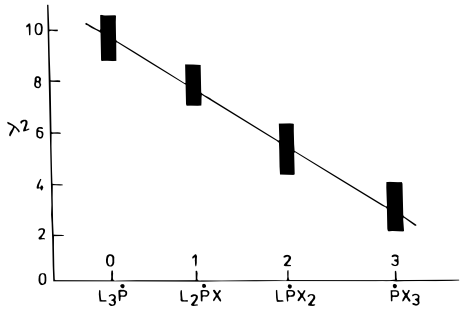

Figure 3. Plot of p/s ratio (λ^2) *vs* number of electronegative ligands (X) in a range of phosphoryl radicals. $\dot{L}_3\dot{P}$, $L_2\dot{P}X_2$, $L\dot{P}X_2$, and $\dot{P}X_3$ where L = H, $\dot{C}H_3$, $CH_3\dot{C}H_2$, or Ph and X = O, S, OH, SH, OCH_3, SCH_3, F, or Cl.

hyperfine data, as the ligands are varied in phosphoranyl radicals. There is a relatively small spread in λ^2 (*ca.* 2.3 ± 1), and errors in estimating the p-orbital component are large, so small trends may be concealed within the errors.

Phosphoryl Radicals. One of the most interesting aspects of the ^{31}P hyperfine coupling constants for phosphoryl radicals is the very large spread in p/s ratios (λ^2) as the ligands vary. This trend is displayed in Figure 3 as a function of the ligands, simply by comparing hydrogen, alkyl or aryl groups, labeled L, with relatively strongly electronegative groups, labeled X. Thus we use data for the $L_3\dot{P}$, $L_2\dot{P}X$, $L\dot{P}X_2$, and $\dot{P}X_3$ species. The results are quite well accommodated by the line shown in Figure 3. The bars, showing the range of data for each group, also contain estimates of errors. These groups are quite well separated so that the plot may have some predictive value. The compounds used are listed in the caption.

In order to understand this clear trend, we invoke the concept of orbital following.[12] This provides an easy route from the p/s ratio (λ^2) to the bond angle for $\dot{A}B_2$ and $\dot{A}B_3$ species.[1] This simple approach has been criticized,[13] but in our view,[14] it is of considerable qualitative use, which is all that is justified in view of the errors in estimating the orbital parameters. There are two accepted ways in which trends in bond angles are qualitatively explained, one being the VSEPR (valence shell electron-pair repulsion) theory,[15] and the other being what we call the "s versus p" theory. In the present case the former theory is not helpful. The latter, however, gives a satisfactory explanation for the observed trends, in our view. This model predicts a planer structure if the SOMO on phosphorus is pure 3p, and *ca.* 90° bond angles if it is pure 3s. The trend to smaller bond angles and smaller λ^2 values as the ligand electronegativities increase is seen as a competition for the s orbital, which has a far higher electron affinity than the p orbitals. The electronegative ligands remove σ electron density from s-p hybrid orbitals and this is minimized by bending since these orbitals then move towards the pure 3p situation for $\Theta = 90°$. This effect competes with the fact that there is, formally, a deficiency of electrons in the SOMO itself. These two effects seem to be well balanced, which explains the large trend, from nearly planar for L = H, or alkyl, to near sp^2 for X = Cl.

These arguments are, of course, quite general for 25-electron $\dot{A}B_3$ species but are very nicely illustrated for these phosphorus derivatives.

An important point is that the same reasoning can be used for the 26-electron closed-shell species ($:AB_3^-$ in this example). This type of argument can be used to give qualitative explanations for bond-angle trends in molecules quite generally and is, in our view, superior, in this pictorial sense, to the more widely used VSEPR (valence shell electron-pair repulsion) theory.[15]

Aspects of Mechanism. *Phosphoranyl Radicals*. For direct electron addition to PL_4 molecules or ions there is a choice for the two limting types of distortion that give either σ^* or TBP structures. The former (σ^*) requires a single bond-stretching mode, while the latter requires a single ABA bond-bending mode. Normally we expect that the most stable species (TBP), would form directly. However, for formation *via* ligand addition to $\dot{P}L_3^+$ radicals (as in (2)) or radical addition to $:PL_3$ molecules (as in (3)), we predict that the σ^* structure will form initially.

$$X: + \dot{P}L_3^+ \rightleftharpoons X\text{-}\dot{\cdot}\text{-}PL_3 \quad (2)$$

$$\dot{X} + :PL_3 \rightleftharpoons X\text{-}\dot{\cdot}\text{-}PL_3 \quad (3)$$

This prediction is based on the principle of microscopic reversibility, and the requirement that the σ^* species be formed as a precursor to the reverse of (2) or (3). It is significant that the σ^* radical PPh_3-$\dot{\cdot}$-SH gave $Ph_3\dot{P}^+$ phosphoryl radicals on annealing,[16] whereas there was no indication of the formation of $Me_3\dot{P}^+$ radicals in the present studies.

Phosphoryl Radicals. The $Me_2\dot{P}S$ radical, formed in good yield, cannot have been derived from the parent phosphoranyl radical by such routes as (2) or (3). In our view, the most probable mechanism for its formation is electron return to give electronically excited $(Me_3PS)^*$ molecules which then undergo bond homolysis as in (4). This an occur by electron transfer

$$(Me_3PS)^* \rightarrow Me^{\bullet} + Me_2\dot{P}S \quad (4)$$

from the radical anions to the cations *via* electron transfer through the lattice. Methyl radical were not detected, but there was an increase in the signal from $H_2\dot{C}P(CH_3)_2S$ radicals on annealing and we suggest that the $\dot{C}H_3$ radicals migrate and react either to give these radicals plus methane, or by adding to sulfur, to give $Me_3\dot{P}SM_3$ centers (species C). Such electron return processes are quite common in the radiolyses of pure compounds.[17]

Librations and Rotations. Here we discuss the two possibly linked processes of methyl group rotation and radical libration. The former is with respect to the molecular frame whilst the latter is with respect to the laboratory frame.

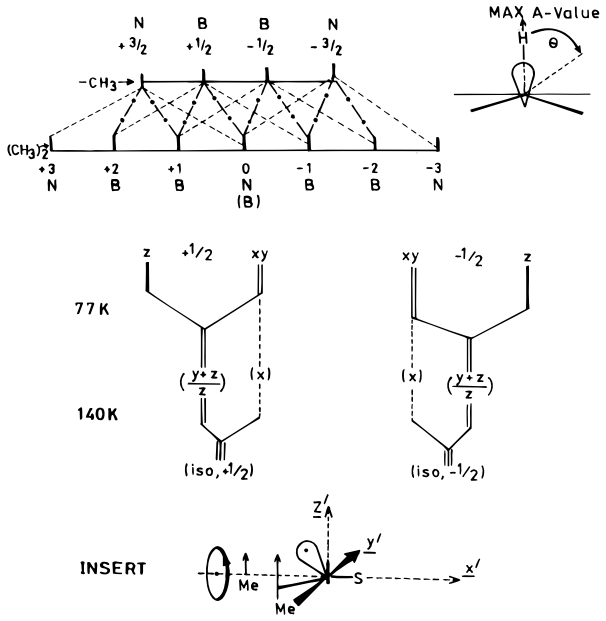

Figure 4. (a, top) Effect of slow and fast rotation of the $-CH_3$ groups: for one $-CH_3$ group, only the sum of the hyperfine splittings (3A) is a constant as the methyl group rotates. Hence only the $|\pm^3/_2>$ lines are well-defined (N). When this is applied to two equivalent methyl groups the $|\pm 3>$ lines are narrow, and part of the $|0>$ feature; the remainder is poorly defined or broad (B), (b, bottom) Change of ($|\pm^1/_2$, ^{31}P) parallel (z) and perpendicular (x, y) features on increasing the temperature. The x features do not move significantly and hence take on the form of "parallel" features. The y and z features average to give perpendicular-like features. The suggested mode of rotation around the P−S bond (x') direction is indicated, together with inversion.

Methyl Group Rotations. As mentioned above, the spectral pattern from the ^{1}H coupling seen in the ^{31}P doublet at 77 K is a 1:2:1 triplet, the overall splitting being 5.7×6 G $= 34.2$ G. This overall splitting remains constant on warming, but broad intermediate lines grow in and narrow such that at *ca*. 140 K there is a normal septet with A(^{1}H) = 5.7 G (Figure 2b).

Thus, the outer $M_I = |\pm 3>$ lines are narrow throughout, together with one component of the $10>$ line, whereas the $|\pm 2>$ and $|\pm 1>$ lines are broadened by restricted rotation of the two $-CH_3$ units relative to the radical frame. This stems from the behavior of each $-CH_3$ interaction for which the $|\pm 3/2>$ features remain narrow while the $|\pm 1/2>$ features are broadened. These combine to give the N,B,B,N,B,B,N pattern observed (see Figure 4a).

This behavior stems from the fact that the hyperfine coupling for each individual proton switches from a maximum when overlap between the C−H bond and the SOMO on phosphorus is maximized to a low value at 90° from this angle. However, the sum for all three protons is a constant for any value for Θ. This is not true for the $M_I = |\pm^1/_2>$ lines, individual components of which vary continuously as Θ varies.

This explains the observed behavior. It is probable that, at low temperatures, rotation is effectively quenched on the EPR time scale. Provided there are no precise orientations that are favored for these groups, the outer lines will remain fixed and defined whereas there will be an infinite number of inner components stemming from all the orbitary orientations so that nothing will be resolved in the intermediate regions, as observed.

Molecular Rotation. In most cases, rotational motions is preceded by librations around the favored site, which lead to partial but uniform averaging of the EPR spectra. These can be understood in terms of the diagram shown in Figure 4b. Thus, using the data derived from these spectra (see Table 1), we have at 77 K, the "true" data for ^{31}P, namely, $A_{||} = 450$ G; $A_\perp = 256$ G with $A_{iso} = 321$ G. At 140 K the apparent values are $A_\perp \simeq 345$ G, $A_{||} = 275$ G, and $A_{iso} = 322$ G. The A_{iso} value agree well, while the new $A_{||}$ is close to the true $A_\perp$ value and the new $A_\perp$ is close to the average of the true parallel and perpendicular values (i.e., *ca*. 353). (The errors involved in these calculations are close to those involved in obtaining good fits to the spectra and are not, in our view, of any significance.)

These changes depicted (Figure 4b) can be approximately accommodated if there is a specific, relatively rapid rotation around the P−S bond direction, as shown in the insert. We suggest that the x axis lies quite close to the P−S direction so that this rotation will not greatly modify A_x, but will average A_y and A_z as required. It may be that a concomitant inversion occurs to give a pseudo planar species.

General Conclusions

There are several aspects of these results that are of general significance.

(i) Should We Use a Double Bond Representation? Two centers, namely the parent cations and the $H_2\dot{C}-PL_3$ centers, have EPR parameters that are very difficult to understand if there is any sort of significant double bonding, as in the representations $L_3P{=}S$ or $L_3P{=}CH_2$, which are almost universally used for each species. We have drawn this conclusion repeatedly in the past,[18,19] but, in recent reviews, all of which claim to confirm the "double bond" concept, the EPR evidence is not even mentioned.[20] In our view, none of the cited evidence for double bond formalism is compelling, nor is the theoretical support particularly strong. Nevertheless, it seems to be normal practice to use the double bond formalism, a representation that seems to be hallowed by usage. It may not mislead practising scientists, but it certainly misled students.

(ii) Use of d-Orbitals. The present results help to confirm our view that there is no measurable, π-delocalization, and σ-π delocalization is trival. Also, the fact that on electron addition, the 3d orbitals are not required to explain the data is significant. The total spin densities for both the σ^* and TBP structures are nicely accounted for just using 3s + 3p atomic orbitals, and major 3d admixture is not required. We urge that the large body of evidence built up over the years using EPR spectroscopy be treated seriously.

(iii) Bond Angles. Although the data for phosphoranyl radicals fail to show a sufficiently clear set of trends as the ligands are varied, the results for phosphoryl radicals show a very large trend. We link the isotropic and anisotropic ^{31}P hyperfine coupling constants with s and p orbital character, and thence link the p/s ratio (λ^2) with bond angle. In this view, as λ^2 increases the radicals move toward a limiting planar structure, favored by covalent or electropositive ligands. As λ^2 falls, the radicals become increasingly pyramidal, and this is induced by electronegative ligands. The simple s versus p competition concept outlined above satisfactorily explains these very large changes.

(iv) Methyl Group Rotation. It is interesting to consider the very marked degree of hindered rotation observed for the methyl groups. This can be compared with the complete absence of any hindrance on the EPR time scale, for the rotation of the methyl groups in planer radicals such as Me_3C.[21,22] This is despite the fact that the H_3C-C bonds are considerably shorter than the H_3C-P bonds. Clearly, it is the movement of the two methyl groups toward each other on bending which leads to the observed restriction of rotation.

All these modes of motion are probably coupled. This would be an interesting system to study from this viewpoint.

Acknowledgment. We thank the Commission of the European Communities for a contract with India supporting this study [CI.1* 0518.M (JR)] and the Leverhulme Trust for financial assistance. Some of this work was carried out in part at the Departments of Chemistry, University of Leicester and University of Essex, U.K.

References and Notes

(1) Breslow, R.; Brandl, M.; Turro, N.; Kassidy, K.; Krogh-Jespersen, K.; Westbrook, J. D. *J. Am. Chem. Soc*. **1987**, *109*, 7204.

(2) Abu-Raqabah, A.; Symons, M. C. R. *J. Am. Chem. Soc*. **1990**, *112*, 8614.

(3) See, for example: Gara, W. B.; Roberts, B. P. *J. Chem. Soc., Perkin Trans. 2* **1978**, 150. Roberts, B. P.; Singh, K. *J. Organomet. Chem*. **1978**, *159*, 31. Davies, A. G.; Parrott, M. J.; Roberts, B. P. *J. Chem. Soc., Chem. Commun*. **1975**, 27. Gilbert, B. C.; Larkin, J. P.; Norman, R. O. C.; Storey, P. M. *J. Chem. Soc., Perkin Trans. 2* **1972**, 1508. Krusic, P. J.; Mahler, W.; Kochi, J. K. *J. Am. Chem. Soc*. **1972**, *94*, 6033.

(4) See, for example: Geoffroy, M.; Lucken, E. A. C. *Mol. Phys*. **1971**, *22*, 257. Kerr, C. M. L.; Webster, K.; Williams, F. *Mol. Phys*. **1973**, *25*, 1461; *J. Phys. Chem*. **1975**, *79*, 2650. Rothuis, R.; Font Friede, J. J. H. M.; Buck, H. M. *Recl. Trav. Chim*. **1973**, *92*, 1308. Begum, A.; Sharp, J. H.; Symons, M. C. R. *J. Chem. Phys*. **1970**, *53*, 3756. Mishra, S. P.; Evans, J. C.; Rowlands, C. C. *J. Inorg. Nucl. Chem*. **1981**, *43*, 481. Colussi, A. J.; Morton, J. R.; Preston, K. F. *J. Chem. Phys*. **1975**, *62*, 2004.

(5) See, for example: Subramanian, S.; Symons, M. C. R.; Wardale, H. W. *J. Chem. Soc. A* **1970**, 1239. Serway, R. A.; Marshall, S. A.; McMillan, J. A.; Marshall, R. L.; Ohlsen, W. D. *J. Chem. Phys*. **1969**, *51*, 4978.

(6) Lyons, A. R.; Symons, M. C. R. *J. Chem. Soc., Faraday Trans. 2* **1972**, 1589.

(7) Symons, M. C. R. *Chem. Soc. Rev*. **1984**, *13*, 393. Shiotani, M. *Magn. Reson. Rev*. **1987**, *12*, 333.

(8) Symons, M. C. R. *Pure Appl. Chem*. **1981**, *53*, 223.

(9) Frocsk, C. *J. Chem. Phys*. **1966**, *45*, 1417. Morton, J.; Preston, K. *J. Magn. Reson*. **1978**, *30*, 577.

(10) Begum, A.; Symons, M. C. R. *J. Chem. Soc., Faraday Trans. 2* **1973**, *69*, 43.

(11) Lyons, A. R.; Neilson, G. W.; Symons, M. C. R. *J. Chem. Soc., Faraday Trans. 2* **1972**, *68*, 1063.

(12) Coulson, C. A. *Vol. Commemortif Victor Henri* **1948**, 15.

(13) Owens, F. J. *Chem. Phys. Lett*. **1973**, *18*, 158. Takahata, Y.; Eri, T.; l'Haya, Y. J. *Chem. Phys. Lett*. **1974**, *26*, 557.

(14) Burton, B.; Claxton, T. A.; Hamshere, S. J.; Marshall, H. E.; Overill, R. E.; Symons, M. C. R. *J. Chem. Soc., Dalton Trans*. **1976**, 2446.

(15) Gillespie, R. J. *Molecular Geometry*; van Nostrand Reinhold: London, 1972. Gillespie, R. J.; Hargittai, I. *The VSEPR Model of Molecular Geometry*; Allyn and Bacon: Boston, 1991.

(16) Eastland, G.; Symons, M. C. R. *J. Chem. Soc., Perkin Trans. 2* **1977**, 833.

(17) Mishra, S. P.; Symons, M. C. R. *Discuss Faraday Chem. Soc*. **1977**, *63*, 175.

(18) Begum, A.; Lyons, A. R.; Symons, M. C. R. *J. Chem. Soc. A* **1971**, 2388.

(19) Rai, U. S.; Symons, M. C. R. *J. Chem. Soc., Faraday Trans*. **1994**, *90*, 2649.

(20) Gilheany, D. G. In *The Chemistry of Organophosphorus Compounds*; Hartley, F. R., Ed.; Wiley: New York, 1992; Vol. II.

(21) Raqabah, A. A.; Symons, M. C. R. *Chem. Phys. Lett*. **1991**, *183*, 171.

(22) Kubota, S.; Matsushita, M.; Shida, T.; Raqabah, A. A.; Symons, M. C. R.; Wyatt, J. L. *Bull. Chem. Soc. Jpn*. **1995**, *68*, 140.